How to cite: *Angew. Chem. Int. Ed.* **2024**, *63*, e202319503
doi.org/10.1002/anie.202319503

Vibrational Spectroscopy

Heterodyne-Detected Sum-Frequency Generation Vibrational Spectroscopy Reveals Aqueous Molecular Structure at the Suspended Graphene/Water Interface

Yongkang Wang[+], Fujie Tang[+], Xiaoqing Yu, Tatsuhiko Ohto, Yuki Nagata, and Mischa Bonn**

Abstract: Graphene, a transparent two-dimensional conductive material, has brought extensive new perspectives and prospects to various aqueous technological systems, such as desalination membranes, chemical sensors, energy storage, and energy conversion devices. Yet, the molecular-level details of graphene in contact with aqueous electrolytes, such as water orientation and hydrogen bond structure, remain elusive or controversial. Here, we employ surface-specific heterodyne-detected sum-frequency generation (HD-SFG) vibrational spectroscopy to re-examine the water molecular structure at a freely suspended graphene/water interface. We compare the response from the air/graphene/water system to that from the air/water interface. Our results indicate that the $\chi^{(2)}_{yyz}$ spectrum recorded from the air/graphene/water system arises from the topmost 1–2 water layers in contact with the graphene, with the graphene itself not generating a significant SFG response. Compared to the air/water interface response, the presence of monolayer graphene weakly affects the interfacial water. Graphene weakly affects the dangling O–H group, lowering its frequency through its interaction with the graphene sheet, and has a very small effect on the hydrogen-bonded O–H group. Molecular dynamics simulations confirm our experimental observation. Our work provides molecular insight into the interfacial structure at a suspended graphene/water interface, relevant to various technological applications of graphene.

The interface of graphene in contact with water and aqueous electrolytes is relevant for many technological applications spanning from water desalination,[1,2] energy storage and conversion,[3–6] chemo-sensing and biosensing,[7] to electrocatalysis.[8] Understanding how graphene affects water molecular structure, such as orientation and hydrogen bond (H-bond) network, is an indispensable prerequisite to comprehending the mechanism of those systems. Such buried interface is optically accessible,[9–11] allowing for surface-specific vibrational spectroscopy such as heterodyne-detected sum frequency generation (HD-SFG) spectroscopy,[10,12] a unique tool capable of selectively probing the orientation and H-bond structure of interfacial water.[13,14] Nevertheless, because of the transparent nature of graphene in terms of substrate-water interactions,[11,15,16] it is challenging to isolate the graphene-water interaction. Indeed, previous HD-SFG spectroscopy of a substrate-supported graphene/water interface demonstrated that the surface chemistry of the supporting substrate governs the interfacial water structure.[17] To avoid the substrate effects, graphene freely suspended on the water surface serves as an alternative platform.[9,12,18] For example, Nagata et al.'s simulations[19] predicted that the water SFG spectrum at the suspended graphene/water interface primarily arises from the topmost few layers of interfacial water and is quite similar to that at the air/water interface with the graphene merely slightly modifying the vibrational frequency of the dangling O–H group of the topmost interfacial water. Subsequently, Laage et al.'s simulations also provided consistent predictions.[18,20] Surprisingly, very recent HD-SFG experimental data by Tian et al.[12] has indicated that the water spectrum at the suspended graphene/water interface might be quite different from the air/water interface, in which graphene itself may contribute to the SFG signal and induce a bulk contribution even under charge-neutral conditions, and both are strong and comparable to the

[*] Y. Wang,[+] X. Yu, Y. Nagata, M. Bonn
Molecular Spectroscopy Department, Max Planck Institute for Polymer Research, Ackermannweg 10, 55128 Mainz, Germany
E-mail: nagata@mpip-mainz.mpg.de
bonn@mpip-mainz.mpg.de

F. Tang[+]
Pen-Tung Sah Institute of Micro-Nano Science and Technology, Xiamen University, 361005 Xiamen, China

F. Tang[+]
Laboratory of AI for Electrochemistry (AI4EC), IKKEM, 361005 Xiamen, China

T. Ohto
Graduate School of Engineering, Nagoya University, Nagoya 464-8603, Japan

[+] Yongkang Wang and Fujie Tang contributed equally to this work.

© 2024 The Authors. Angewandte Chemie International Edition published by Wiley-VCH GmbH. This is an open access article under the terms of the Creative Commons Attribution License, which permits use, distribution and reproduction in any medium, provided the original work is properly cited.

© 2024 The Authors. Angewandte Chemie International Edition published by Wiley-VCH GmbH

contribution from interfacial water. Given the vast divergence between the simulations and experimental data from different research groups and the profound relevance of the graphene/water interface in numerous technological applications, it is crucial to re-examine the molecular structure at the graphene/water interface to elucidate the extent and depth that graphene interacts with water across the interface.

Here, we apply HD-SFG spectroscopy to the suspended graphene/water interface to re-examine its interfacial molecular structure. By comparing the experimental data with *ab initio* molecular dynamics (AIMD) as well as the machine learning force field MD (MLFF-MD) simulation data, we identify the molecular origin of the interfacial water SFG spectrum at the suspended graphene/water interface. Our results reveal that monolayer graphene itself does not generate a significant SFG response, and the measured $\chi^{(2)}_{yyz}$ spectrum at the suspended graphene/water interface arises from the topmost interfacial water in contact with the graphene. From the comparison with the spectrum at the air/water interface, we further demonstrate that the presence of a monolayer graphene weakly affects the interfacial water structure. Graphene modifies the dangling O–H peak frequency through the interactions of the dangling O–H group with the graphene sheet, including van der Waals (vdW) interaction and the interaction of the hydrogen atom of the O–H group with the π-orbital of the graphene sheet.[19] In contrast, graphene has little impact on the topmost interfacial water's hydrogen-bonded (H-bonded) O–H group. Our work provides molecular insights into the interfacial structure at a graphene/water interface, relevant for various technological applications such as water desalination membranes, chemosensing, biosensing, energy storage, and energy conversion devices.

To generate the air/graphene/water system, a commercially available CVD-grown graphene sheet on copper foil was exposed to a 10 mM ammonium persulfate (APS) solution to etch away the copper foil. Once etched, the APS solution was diluted repeatedly with pure water (see Section S1–S3 of the *Supporting Information* for details). Using this method, centimeter-scale monolayer graphene suspended on the water surface was obtained (Figure 1A and SI-Figure S1). To check the graphene quality, we measured the Raman spectrum (Figure 1B). The absence of the defect-related Raman D-band (~1350 cm^{-1}) indicates that the graphene remains intact and of high quality.[21] The 2D-band (~2679 cm^{-1}) and G-band (~1585 cm^{-1}) intensity ratio of ~3 confirms that the graphene is present as a monolayer. Furthermore, the ~1585 cm^{-1} G-band frequency suggests the suspended graphene is very weakly charged (undoped) in contact with water with a negligible charge density of < 0.5 mC/m^2.[9]

Figure 1C shows the HD-SFG measurements on the suspended graphene sample using the *ssp* polarization combination (with the three letters indicating the polarization of the SFG, visible, and infrared, respectively). To avoid water present on the air side of the graphene and to avoid spectral distortion due to water vapor in the air, HD-

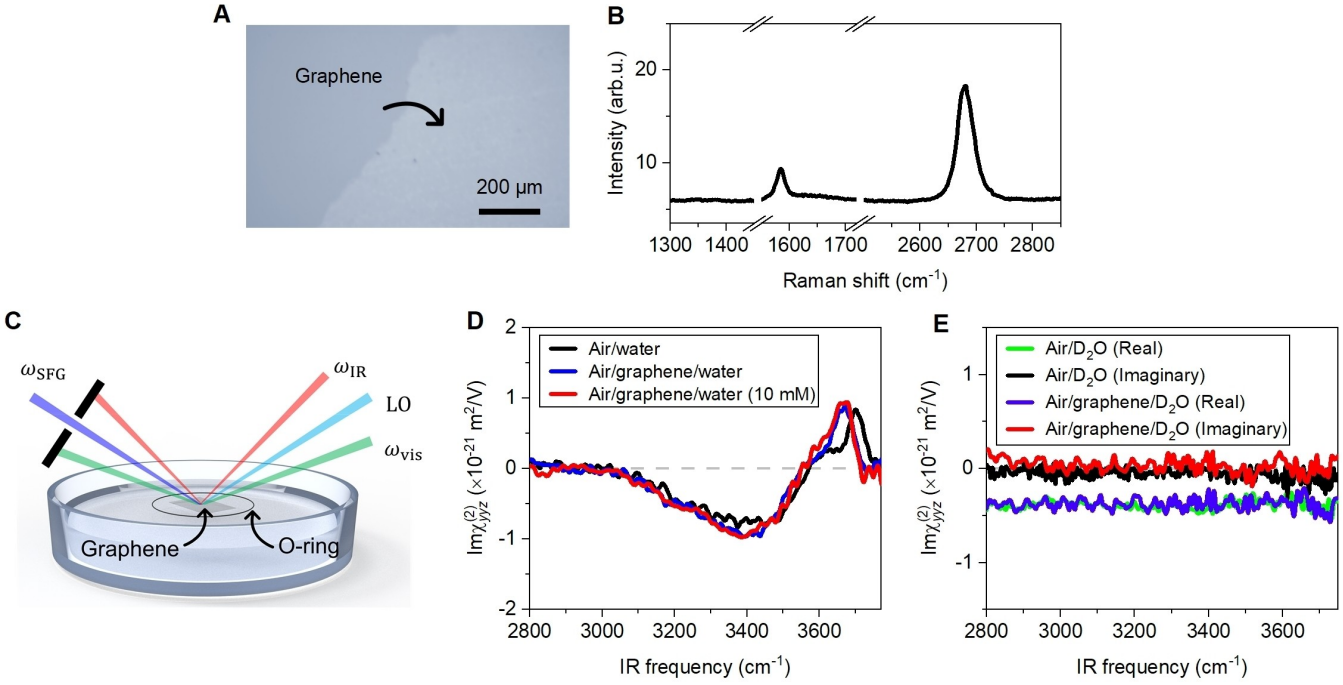

Figure 1. HD-SFG detection of water at a suspended graphene/water interface. (**A**). An optical image of the suspended graphene on the water surface. (**B**). The Raman spectrum of the graphene suspended on the water surface is consistent with defect-free, undoped monolayer graphene. (**C**). Experimental setup for the HD-SFG measurements. (**D**). The $\mathrm{Im}\chi^{(2)}_{yyz}$ spectra of the air/water interface (black), suspended graphene/water interface before (blue) and after (red) adding with 10 mM NaCl. (**E**). The real and imaginary parts of the $\chi^{(2)}_{yyz}$ spectra at the air/D_2O interface and the suspended graphene/D_2O interface. The dashed lines in (**D**) and (**E**) are zero lines.

© 2024 The Authors. Angewandte Chemie International Edition published by Wiley-VCH GmbH

15213773, 2024, 20, Downloaded from https://onlinelibrary.wiley.com/doi/10.1002/anie.202319503 by MPI 355 Polymer Research, Wiley Online Library on [16/05/2024]. See the Terms and Conditions (https://onlinelibrary.wiley.com/terms-and-conditions) on Wiley Online Library for rules of use; OA articles are governed by the applicable Creative Commons License

SFG measurements were conducted in a dried-air atmosphere (RH < 3 %). The obtained $\mathrm{Im}\chi^{(2)}_{yyz}$ spectrum after correcting for the reflectivity and Fresnel factors (See SI-Section S4)[22,23] is displayed in Figure 1D. The $\mathrm{Im}\chi^{(2)}_{yyz}$ spectrum exhibits a negative 3400 cm^{-1} broad peak and a high-frequency positive 3670 cm^{-1} peak. The negative 3400 cm^{-1} peak arises from the H-bonded O–H stretch mode of water at the suspended graphene/water interface.[18,19] Its negative sign means the H-bonded O–H group points down towards the bulk water.[13] We note that the 3400 cm^{-1} peak appears with almost the same frequency and amplitude at the air/water interface (Figure 1D), implying that graphene only weakly affects the organization of the interfacial water. We emphasize that the air/water spectrum was obtained utilizing the diluted etchant transferred from the graphene/water sample. This spectrum demonstrates minimal variance when compared to the spectrum acquired using pure water (SI-Section S5), suggesting the purity of the diluted etchant. Additionally, the lack of C–H stretch peaks (2850–2950 cm^{-1}) in these spectra further underscores the cleanliness of the samples.

The high-frequency peak at the suspended graphene/water interface is slightly red-shifted compared to the air/water interface. It has the same sign and almost the same amplitude, but its frequency of 3670 cm^{-1} is lower compared to the 3700 cm^{-1} peak at the air/water interface. The 3700 cm^{-1} peak at the air/water interface arises from the "dangling O–H" group, pointing out towards the vapor phase, not hydrogen bonding with other water.[24] The frequency redshift of the dangling OH peak at the suspended graphene/water interface implies a weak, but non-negligible interaction of the dangling O–H with the graphene. Indeed, previous molecular dynamics simulations have predicted the O–H peak as the O–H stretch chromophore interacting with the π-orbital of the graphene sheet.[19] The O–H group points up to the graphene sheet and into the vacuum between water and the graphene, and therefore has a positive sign.[18,19] We stress that the redshift of approximately 30 ± 10 cm^{-1} in the frequency of the water dangling O–H peak at the graphene/water interface, relative to the air/water interface, aligns with the behavior of water at the benzene/water interface (SI-Section S6).

At a charged interface, in addition to the surface contribution arising from the alignment of the topmost 1–2 water layers, the penetration of the electrostatic field into the bulk solution induces alignment and polarization of water molecules in the diffuse layer, providing a bulk contribution to the $\chi^{(2)}_{yyz}$ spectrum.[25–27] To check for a bulk contribution at a pristine suspended graphene/water interface, we measured the $\chi^{(2)}_{yyz}$ spectrum at the suspended graphene/water interface by adding NaCl (10 mM) to the water. The addition of electrolyte screens the surface charge, and the bulk contributions to the SFG spectrum (if present) should be significantly modified, while the surface contribution remains unaffected.[25] The data is shown in Figure 1D. Within experimental uncertainty, the two $\mathrm{Im}\chi^{(2)}_{yyz}$ spectra are indistinguishable, indicating no bulk contribution exists at the suspended graphene/water interface,[20,25] consistent with the Raman data that the suspended graphene on the water surface is very weakly charged (Figure 1B).

Furthermore, to explore whether monolayer graphene generates a SFG response, we measured the $\chi^{(2)}_{yyz}$ spectrum at the suspended graphene/D_2O interface and compared it with the $\chi^{(2)}_{yyz}$ spectrum at the air/D_2O interface. As D_2O has no resonance in the O–H stretching region, the $\chi^{(2)}_{yyz}$ spectrum at the air/D_2O interface is purely real, and its imaginary part is zero (Figure 1E).[28] The $\chi^{(2)}_{yyz}$ spectrum at the suspended graphene/D_2O interface is also pure real, with the same value as that at the air/D_2O interface. This unequivocally demonstrates that monolayer graphene itself does not generate an SFG response. We emphasize that the negligible sum-frequency response from monolayer graphene is consistent with previous studies collected at supported graphene/water interface on different substrates,[10,16,29,30] and suspended graphene/water interface in contact with different electrolyte solutions.[9] These results suggest that the measured $\chi^{(2)}_{yyz}$ spectrum at the suspended graphene/water interface mainly arise from the topmost interfacial water in contact with the graphene.

A weakly affected $\mathrm{Im}\chi^{(2)}_{yyz}$ spectrum of water in contact with the monolayer graphene contrasts with recent experimental work[12] in the following three points. First, the SFG amplitude at the graphene/water interface was almost half of the SFG amplitude at the air/water interface in Ref. [12], while we find that the SFG amplitudes are similar. Second, the frequency of the dangling O–H peak was red-shifted by ~100 cm^{-1} at the graphene/water interface compared with the air/water interface in Ref. [12], while we find that the redshift is 30 ± 10 cm^{-1}. Third, we do not find a strong background from the graphene sheet, in contrast with Ref. [12].

To resolve the controversy of the SFG amplitudes and the frequency shift of the dangling O–H peak, we carried out the AIMD simulation of the graphene/water/air system at the BLYP + D3 level of theory[19] and computed the $\chi^{(2)}_{yyz}$ spectra via the surface-specific velocity-velocity correlation function formalism.[31] Note that the intermolecular/intramolecular couplings of the O–H stretch mode were not included in the simulation. The simulation details are given in SI-Section S7. The snapshots of the simulated air/water and graphene/water interfaces are shown in Figure 2A. The corresponding number density profiles are given in Figure 2B. We observe that the density of water oscillates near the graphene sheet, while it is flat in the $12\ \text{Å} < z < 17\ \text{Å}$ region which is considered as the bulk region.

The simulated SFG spectra are shown in Figure 2C. The simulated spectra show similar SFG amplitudes of water at the graphene/water and air/water interfaces and a 50 ± 7 cm^{-1} redshift of the dangling O–H peak at the graphene/water, consistent with the experimental data. To confirm that this observation is independent of the choice of the density functional theory level, we further carried the machine-learning force field (MLFF)-MD simulation at the revPBE + D3 level of theory.[32–34] The calculated spectra at the revPBE + D3 level of theory are displayed in Figure 2D. Similarly, we found similar SFG amplitudes at the graphene/water and air/water interfaces as well as the redshift of 30 ±

© 2024 The Authors. Angewandte Chemie International Edition published by Wiley-VCH GmbH

15213773, 2024, 20, Downloaded from https://onlinelibrary.wiley.com/doi/10.1002/anie.202319503 by MPI 355 Polymer Research, Wiley Online Library on [16/05/2024]. See the Terms and Conditions (https://onlinelibrary.wiley.com/terms-and-conditions) on Wiley Online Library for rules of use; OA articles are governed by the applicable Creative Commons License

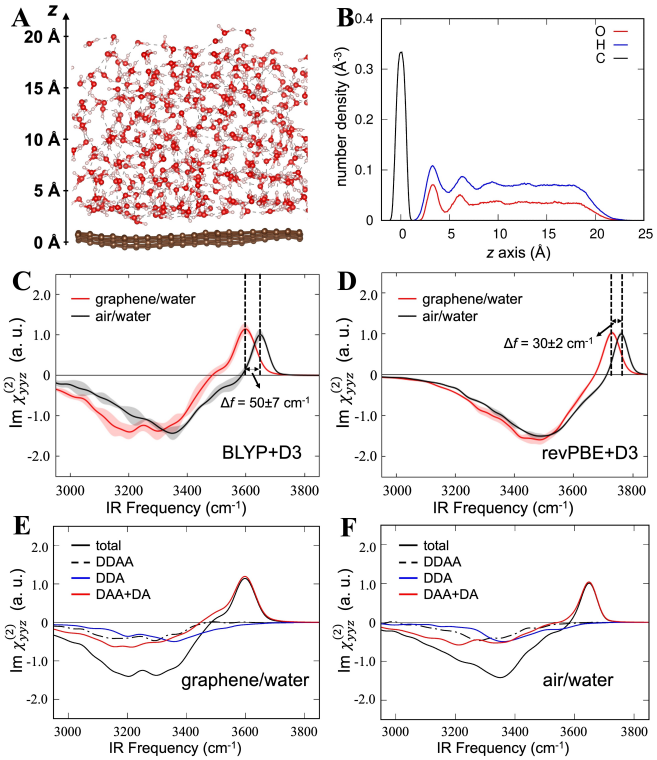

Figure 2. AIMD and MLFF-MD simulations of the air/water interface and the suspended graphene/water interface. (**A**) Snapshot of the AIMD simulation trajectory. The upper and lower interfaces are the air/water interface and the suspended graphene/water interface, respectively. (**B**) The number density profiles of the oxygen, hydrogen, and carbon atoms along the surface normal (*z*-axis) based on the AIMD simulation trajectory.[19] The origin point of the *z-axis* was set to the center of mass for the graphene sheet. (**C**) Simulated $\mathrm{Im}\chi^{(2)}_{yyz}$ spectra of the suspended graphene/water interface and the air/water interface based on the AIMD simulation trajectory at the BLYP + D3 level of theory.[19] (**D**) Simulated $\mathrm{Im}\chi^{(2)}_{yyz}$ spectra based on the MLFF-MD simulation trajectory at the revPBE + D3 level of theory. The shadow areas in **C** and **D** indicate the 95 % confidence intervals. (**E**, **F**) Corresponding DA, DAA, DDA, and DDAA water species at (**E**) the suspended graphene/water interface and (**F**) the air/water interface based on the AIMD trajectory at the BLYP + D3 level of theory.

2 cm^{-1}. Again, this observation is consistent with our experimental data, but at odds with the data in Ref. [12].

To further examine the conformation of the interfacial water molecules, we decomposed the SFG spectra of the interfacial water into those from the different H-bond species of water.[35] Note that we used the H-bond definition rather than the free O–H definition,[36] because the free O–H definition is fully optimized to identify the free O–H group at the air/water interface and thus it is not appropriate for the graphene/water interface. In this context, the notation "D" signifies a water molecule containing a donor H-bond, while "A" denotes the presence of an acceptor H-bond, we used the H-bond definition developed in Ref. [35]. The decomposed SFG data at the graphene/water and air/water interfaces are depicted in Figure 2E and Figure 2F (see SI-Section S8 for details). As expected, at both of the two interfaces, the contributions for the high-frequency dangling O–H peak mainly come from the "DAA + DA" species, located in the topmost water layer near the interfacial regions. Notably, for all different species including "DDAA", "DDA", and "DAA + DA", the presence of the graphene sheet very weakly affects their relative peak amplitudes and contributions. As a result, the SFG amplitudes of the dangling O–H peak and H-bonded O–H peak show an almost insensitive behavior to the presence and absence of the graphene sheet. The presence of the graphene only affects the dangling O–H peak coming from the "DAA + DA" species, by lowering its frequency through its interaction with the graphene sheet via the vdW interaction and O–H-π interaction, showing that the graphene interacts mainly with the topmost interfacial water in contact with the graphene. The decomposition of the SFG spectra demonstrates that the graphene only weakly affects the topmost interfacial water. It affects the dangling O–H group, lowering its frequency, and has a very small effect on the hydrogen-bonded O–H group.

Our work demonstrates that monolayer graphene itself does not generate an SFG response. Given its transparent nature, allowing for optical access to the buried graphene/water interface, the graphene electrode serves as an ideal platform for surface-specific HD-SFG vibrational spectroscopy of the electrode/aqueous electrolyte interface. HD-SFG spectroscopy of the suspended graphene/water interface demonstrates a weak interaction of suspended graphene with interfacial water, consistent with our previous HD-SFG spectroscopy of substrate-supported graphene electrode/aqueous electrolyte interfaces.[10,16,17] We stress that the observed negligible bulk contribution and negligible graphene SFG response are consistent with previous studies from different research groups[9,10,29,30] but contrast with recent experimental work,[12] implying that the origins of these two contributions reported in their work should be reevaluated. Our work complements our molecular-level understanding of the graphene/aqueous electrolyte interface, relevant for various technological applications of graphene, such as water desalination, chemo-sensing, biosensing, energy storage and conversion, and neuromorphic iontronics.

Supporting Information

More details about the suspended graphene sample preparation/characterization, Raman, and HD-SFG measurements can be found in Sections S1–S4 of the *Supporting Information*. Discussions on the cleanliness of the suspended graphene sample and graphene-water interaction were included in SI-Sections S5–S6. Additional results regarding the AIMD and MLFF-MD simulations are given in SI-Sections S7–S8.

Acknowledgements

We are grateful for the financial support from the Max-Water Initiative of the Max Planck Society. Funded by the

© 2024 The Authors. Angewandte Chemie International Edition published by Wiley-VCH GmbH

15213773, 2024, 20, Downloaded from https://onlinelibrary.wiley.com/doi/10.1002/anie.202319503 by MPI 355 Polymer Research, Wiley Online Library on [16/05/2024]. See the Terms and Conditions (https://onlinelibrary.wiley.com/terms-and-conditions) on Wiley Online Library for rules of use; OA articles are governed by the applicable Creative Commons License

European Union (ERC, n-AQUA, 101071937). Views and opinions expressed are however those of the author(s) only and do not necessarily reflect those of the European Union or the European Research Council Executive Agency. Neither the European Union nor the granting authority can be held responsible for them. F.T. is supported by a startup fund at Xiamen University. Part of this work used the computational resources in the IKKEM intelligent computing center. Open Access funding enabled and organized by Projekt DEAL.

Conflict of Interest

The authors declare no conflict of interest.

Data Availability Statement

The data that support the findings of this study are available from the corresponding author upon reasonable request.

Keywords: HD-SFG spectroscopy · Interfacial water · Graphene · Ab initio molecular dynamics

[1] M. Heiranian, A. B. Farimani, N. R. Aluru, *Nat. Commun.* **2015**, *6*, 8616.
[2] S. P. Surwade, S. N. Smirnov, I. V. Vlassiouk, R. R. Unocic, G. M. Veith, S. Dai, S. M. Mahurin, *Nat. Nanotechnol.* **2015**, *10*, 459–464.
[3] Z. Li, S. Gadipelli, H. Li, C. A. Howard, D. J. Brett, P. R. Shearing, Z. Guo, I. P. Parkin, F. Li, *Nat. Energy* **2020**, *5*, 160–168.
[4] S. Boyd, K. Ganeshan, W.-Y. Tsai, T. Wu, S. Saeed, D. Jiang, N. Balke, A. C. T. van Duin, V. Augustyn, *Nat. Mater.* **2021**, *20*, 1689–1694.
[5] J. Cai, E. Griffin, V. H. Guarochico-Moreira, D. Barry, B. Xin, M. Yagmurcukardes, S. Zhang, A. K. Geim, F. M. Peeters, M. Lozada-Hidalgo, *Nat. Commun.* **2022**, *13*, 5776.
[6] J. Chmiola, G. Yushin, Y. Gogotsi, C. Portet, P. Simon, P. L. Taberna, *Science* **2006**, *313*, 1760–1763.
[7] Y. Wang, T. Seki, P. Gkoupidenis, Y. Chen, Y. Nagata, M. Bonn, *Proc. Nat. Acad. Sci.* **2024**, *121*, e2314347121.
[8] I. Ledezma-Yanez, W. D. Z. Wallace, P. Sebastián-Pascual, V. Climent, J. M. Feliu, M. T. M. Koper, *Nat. Energy* **2017**, *2*, 17031.
[9] S. Yang, X. Zhao, Y.-H. Lu, E. S. Barnard, P. Yang, A. Baskin, J. W. Lawson, D. Prendergast, M. Salmeron, *J. Am. Chem. Soc.* **2022**, *144*, 13327–13333.
[10] Y. Wang, T. Seki, X. Liu, X. Yu, C.-C. Yu, K. F. Domke, J. Hunger, M. T. M. Koper, Y. Chen, Y. Nagata, M. Bonn, *Angew. Chem. Int. Ed.* **2023**, *62*, e202216604.
[11] D. Kim, E. Kim, S. Park, S. Kim, B. K. Min, H. J. Yoon, K. Kwak, M. Cho, *Chem* **2021**, *7*, 1602–1614.
[12] Y. Xu, Y.-B. Ma, F. Gu, S.-S. Yang, C.-S. Tian, *Nature* **2023**, *621*, 506–510.
[13] S. Nihonyanagi, S. Yamaguchi, T. Tahara, *J. Chem. Phys.* **2009**, *130*, 204704.
[14] Y. R. Shen, *Annu. Rev. Phys. Chem.* **2013**, *64*, 129–150.
[15] C.-J. Shih, M. S. Strano, D. Blankschtein, *Nat. Mater.* **2013**, *12*, 866–869.
[16] Y. Wang, Y. Nagata, M. Bonn, *Faraday Discuss.* **2024**, *249*, 303–316.
[17] Y. Wang, T. Seki, X. Yu, C.-C. Yu, K.-Y. Chiang, K. F. Domke, J. Hunger, Y. Chen, Y. Nagata, M. Bonn, *Nature* **2023**, *615*, E1–E2.
[18] Y. Zhang, H. B. de Aguiar, J. T. Hynes, D. Laage, *J. Phys. Chem. Lett.* **2020**, *11*, 624–631.
[19] T. Ohto, H. Tada, Y. Nagata, *Phys. Chem. Chem. Phys.* **2018**, *20*, 12979–12985.
[20] J.-F. Olivieri, J. T. Hynes, D. Laage, *Faraday Discuss.* **2024**, *249*, 289–302.
[21] X. Liang, B. A. Sperling, I. Calizo, G. Cheng, C. A. Hacker, Q. Zhang, Y. Obeng, K. Yan, H. Peng, Q. Li, X. Zhu, H. Yuan, A. R. Hight Walker, Z. Liu, L. Peng, C. A. Richter, *ACS Nano* **2011**, *5*, 9144–9153.
[22] X. Yu, K.-Y. Chiang, C.-C. Yu, M. Bonn, Y. Nagata, *J. Chem. Phys.* **2023**, *158*, 044701.
[23] X. Zhuang, P. B. Miranda, D. Kim, Y. R. Shen, *Phys. Rev. B* **1999**, *59*, 12632–12640.
[24] V. Ostroverkhov, G. A. Waychunas, Y. R. Shen, *Phys. Rev. Lett.* **2005**, *94*, 046102.
[25] Y.-C. Wen, S. Zha, X. Liu, S. Yang, P. Guo, G. Shi, H. Fang, Y. R. Shen, C. Tian, *Phys. Rev. Lett.* **2016**, *116*, 016101.
[26] S. K. Reddy, R. Thiraux, B. A. Wellen Rudd, L. Lin, T. Adel, T. Joutsuka, F. M. Geiger, H. C. Allen, A. Morita, F. Paesani, *Chem* **2018**, *4*, 1629–1644.
[27] P. E. Ohno, H. Wang, F. M. Geiger, *Nat. Commun.* **2017**, *8*, 1032.
[28] S. Nihonyanagi, R. Kusaka, K. Inoue, A. Adhikari, S. Yamaguchi, T. Tahara, *J. Chem. Phys.* **2015**, *143*, 124707.
[29] A. Montenegro, C. Dutta, M. Mammetkuliev, H. Shi, B. Hou, D. Bhattacharyya, B. Zhao, S. B. Cronin, A. V. Benderskii, *Nature* **2021**, *594*, 62–65.
[30] S. Singla, E. Anim-Danso, A. E. Islam, Y. Ngo, S. S. Kim, R. R. Naik, A. Dhinojwala, *ACS Nano* **2017**, *11*, 4899–4906.
[31] T. Ohto, K. Usui, T. Hasegawa, M. Bonn, Y. Nagata, *J. Chem. Phys.* **2015**, *143*, 124702.
[32] J. P. Perdew, K. Burke, M. Ernzerhof, *Phys. Rev. Lett.* **1996**, *77*, 3865–3868.
[33] Y. Zhang, W. Yang, *Phys. Rev. Lett.* **1998**, *80*, 890.
[34] S. Grimme, J. Antony, S. Ehrlich, H. Krieg, *J. Chem. Phys.* **2010**, *132*, 154104.
[35] A. Vila Verde, P. G. Bolhuis, R. K. Campen, *J. Phys. Chem. B* **2012**, *116*, 9467–9481.
[36] F. Tang, T. Ohto, T. Hasegawa, W. J. Xie, L. Xu, M. Bonn, Y. Nagata, *J. Chem. Theory Comput.* **2018**, *14*, 3363–3363.

Manuscript received: December 17, 2023
Accepted manuscript online: March 13, 2024
Version of record online: April 11, 2024

© 2024 The Authors. Angewandte Chemie International Edition published by Wiley-VCH GmbH

15213773, 2024, 20, Downloaded from https://onlinelibrary.wiley.com/doi/10.1002/anie.202319503 by MPI 355 Polymer Research, Wiley Online Library on [16/05/2024]. See the Terms and Conditions (https://onlinelibrary.wiley.com/terms-and-conditions) on Wiley Online Library for rules of use; OA articles are governed by the applicable Creative Commons License